IJREAT International Journal of Research in Engineering & Advanced Technology, Volume 5, Issue 5, Oct - Nov, 2017
ISSN: 2320 – 8791 (Impact Factor: 2.317)
www.ijreat.org

Impact Of Chemical Reaction And Suction/Injection Over Porous Vertical Cone Filled With Nanofluid

P. Sreedevi[1], K.V. Suryanarayana Rao[2]

[1]Research Scholar, Department of Mathematics, Rayalaseema University, Kurnool, AP, India.

[2]Dept. of Mathematics, RGM College of Eng.& Technology, Nandyal, AP, India.

Abstract:

In this article we have presented MHD natural convection boundary layer heat and mass transfer flow over a vertical coneembedded in porous medium filled with nanofluidunder the enhanced boundary conditions in the presence of thermal radiation, chemical reaction and suction/injection. The transformed conservation equations together with boundary conditions are then solved numerically by using versatile, extensively validated, variational finite element method. The influence of key parameters on velocity, temperature and concentration evaluation in the boundary layer region are examined in detail. Furthermore, the effect of these parameters on local skin friction coefficient (C_f), local Nusselt number (Nu_x) and local Sherwood number (Sh_x) is also investigated.

Keywords: *Vertical Cone; Brownian motion; Thermophoresis; Chemical Reaction; Suction/Injection; Finite Element Method.*

1. Introduction

The thermal conductivity of the base fluids can be enhanced by suspending nanometer sized (1 – 100 nm) particles into it. This suspension of nanoparticles into the base fluids creates a new fluid called nanofluid.The theory of nanofluid was first introduced by Choi et al.[1] while doing research on new coolants and cooling technologies. The thermal conductivity and ultra - small particle size are the very valuable thermophysical properties of nanofluids, because of this nanofluids shows significantly better performance than the normal single - phase and multi-phase fluids [2, 3]. We can found many experimental and numerical studies in literature to know the importance of nanofluid natural convection heat transfer [4, 5]. In his bench mark study, Buongiorno et al. [6] has reported seven possible mechanisms associating nanofluid natural convection through moment of nanoparticles in the base fluid using scale analysis. Brownian motion and thermophoresis are the heat and mass transfer mechanisms, which affect the convective heat transfer performance of nanofluids[7].Kuznetsovand Nield[8] have discussed the influence of Brownian motion and thermophoresis on nanofluid natural convection boundary layer flow over a vertical plate under the enhanced boundary conditions. Aziz and Khan[9] have presented nanofluid natural convection boundary layer flow over a vertical plate subject to the convective boundary conditions. Chamkha et al. [10] studied the mixed convection MHD flow of a nanofluid past a stretching permeable surface in the presence of Brownian motion and thermophoresis effects. Rashidi et al. [11] discussed the dynamics of nanofluid from a non-linearly stretching sheet with transpiration using Homotopy simulation. Noghrehabadi and Behseresht[12] have analyzed how flow and heat transfer are affected by variable properties of nanofluid over a vertical cone saturated in a porous medium. Noghrehabadi et al. [13] have analyzed the natural convection of nanofluids under different geometries like, stretching sheet, vertical plate respectively.Sudarsana Reddy and SuryanarayanaRao [14] reported the influence of magnetic field and chemical reaction on Al_2O_3 - water and Ag - water nanofluids over a vertical cone. Behseresht et al. [15] have presented natural convection heat and mass transfer of nanofluid over a vertical cone by taking the practical range of nanofluids thermo-physical properties. Gorla et al. [16] have studied nanofluid natural convection boundary layer flow through porous medium over a vertical cone. Chamkha et al. [17] were presented non-Darcy free convective nanofluid along a vertical plate with suction/injection and internal heat generation. Chamkha et al. [18] have investigated Non-Newtonian nanofluid natural convection flow over a cone through porous medium with uniform heat and volume fraction fluxes. Garrosi et al. [19] have presented natural convection of nanofluids in square cavity and heat exchangers respectively.Sudarsana Reddy *et al.* [20] presented the influence of size, shape, type of nanoparticles, type and temperature of the base fluid on MHD natural convection of nanofluids over a stretching sheet.Ruchika et al. [21]have presented the influence of velocity and thermal slip effects on MHD boundary layer flow of nanofluid over an inclined cylinder.Haile and Sankar [22] perceived the impact of convective boundary condition on nanofluid flow over a stretching sheet embedded in porous media with radiation, magnetic field and viscous dissipation.

2. Mathematical Analysis

Fig.1 demonstrates a two-dimensional, study, electrically conducting heat and mass transfer boundary layer flow of nanofluid over a vertical cone. The coordinate system is chosen as the *x*-axis is coincident with the flow direction over the cone surface. It is assumed that T_w , is the temperature at the surface of the cone ($y=0$), the concentration of nanoparticles at the surface of the cone is controlled by the condition $D_B \frac{\partial C}{\partial y} + \left(\frac{D_T}{T_\infty}\right)\frac{\partial T}{\partial y} = 0$ and T_∞ , C_∞ are the temperature and concentration of nanoparticles of the ambient fluid, respectively. An external magnetic field of strength B_0 is applied in the direction of the *y*-axis. By considering the works of Kuznetsov and Nield [8] and by employing the Oberbeck - Boussinesq approximation the governing equations describing the steady-state conservation of mass, momentum, energy as well as conservation of nanoparticles for nanofluids in the presence of thermal radiation and other important parameters take the following form:

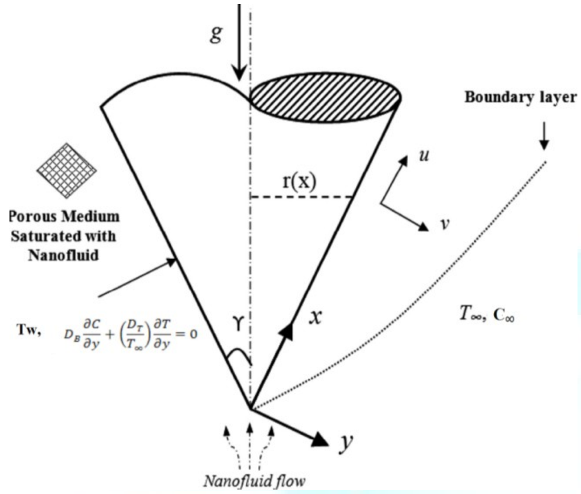

Fig. 1.Physical model and coordinate system.

$$\frac{\partial(ru)}{\partial x}+\frac{\partial(rv)}{\partial y}=0 \quad (1)$$

$$u\frac{\partial u}{\partial x}+v\frac{\partial u}{\partial y}=\nu\frac{\partial^2 u}{\partial y^2}-\frac{\mu}{\rho k}u+g\left[(1-C_\infty)\rho_{f\infty}\beta(T\right. \quad (2)$$

$$u\frac{\partial T}{\partial x}+v\frac{\partial T}{\partial y}=\alpha\frac{\partial^2 T}{\partial y^2}+\tau\left[D_B\frac{\partial C}{\partial y}.\frac{\partial T}{\partial y}+\left(\frac{D_T}{T_\infty}\right)\left(\frac{\partial}{\partial}\right.\right. \quad (3)$$

$$u\frac{\partial C}{\partial x}+v\frac{\partial C}{\partial y}=D_B\frac{\partial^2 C}{\partial y^2}+\left(\frac{D_T}{T_\infty}\right)\frac{\partial^2 T}{\partial y^2} \quad (4)$$

The associated boundary conditions are

$$u=0, v=V_w, T=T_w, j_p=0\, at\, y=0 \quad (5)$$

$$u\to 0, T\longrightarrow T_\infty, C\longrightarrow C_\infty\, t\, y\to\infty \quad (6)$$

Where, $j_p=-D_B\nabla\phi-D_T\frac{\nabla T}{T}$, is the drift-flux model of nanoparticles. Furthermore, the concentration boundary condition at $y=0$ is taken as $j_p=0$.

We now introduce the following similarity variables to transform the governing equations into system of ordinary differential equations:

$$\eta=\frac{y}{x}Ra_x^{\frac{1}{4}}, f(\eta)=\frac{\psi}{\alpha Ra_x^{\frac{1}{4}}}, \theta(\eta)=\frac{T-T_\infty}{T_w-T_\infty},$$

$$\phi(\eta)=\frac{C-C_\infty}{C_w-C_\infty} \quad (7)$$

where, $g\beta\frac{\rho_{f\infty}(¿¿w-T_\infty)(1-C_\infty)Cos\gamma x^3}{\mu\alpha}$ T , $Ra_x=¿$

is the Rayleigh number.

Here, r can be approximated by the local radius of the cone, if the thermal boundary layer is thin, and is related to the *x* coordinate by $r=x\,sin\gamma$.

Using the above similarity variables the equations (1) - (4) takes the form

$$f'''-\frac{1}{Pr}\left(\frac{1}{2}(f')^2-\frac{3}{4}ff''\right)+(\theta-Nr\phi)-Kf'-Mf'=0 \quad (8)$$

$$\theta'' + \frac{3}{4} f\theta' + Nb\,\theta'\phi' + Nt(\theta')^2 = 0 \qquad (9)$$

$$\phi'' + \frac{3}{4} \le f\phi' + \frac{Nt}{Nb}\theta'' = 0 \qquad (10)$$

The transformed boundary conditions are

$$\eta = 0, f = V0, f' = 1, \theta = 1, Nb\,\phi' + Nt\,\theta' = 0.$$

$$\eta \longrightarrow \infty, f' = 0, \theta = 0, \phi = 0. \qquad (11)$$

where, prime denotes differentiation with respect to η, and the significant thermophysical parameters dictating the flow dynamics are defined by

$$C\;T\;C\;T$$

$$\tau D_T \frac{(¿¿w - T_\infty)}{\alpha T_\infty}, \le ¿ \frac{\alpha}{D_B}, K = \frac{x^2}{k\,Ra_x^{\frac{1}{2}}}, Pr = \frac{\mu}{\rho\alpha}, \backslash$$

$$\tau D_B \frac{(¿¿w - C_\infty)}{\alpha}, Nt = ¿$$

$$\rho_{f\infty}\beta(¿¿w - T_\infty)(1 - C_\infty), N$$

$$(\rho_p - \rho_{f\infty})\frac{(¿¿w - C_\infty)}{¿}$$

$$Nr = ¿$$

(12)

Where, $f(0) = V0$, with $V0 > 0$ corresponds to suction and $V0 < 0$ represents injection.

Quantities of practical interest in this problem are the skin-friction coefficient, local Nusselt number Nu_x, and the local Sherwood number Sh_x, which are defined as

$$C_f = \frac{2\tau_w}{\rho}, Nu_x = \frac{xq_w}{k(T_w - T_\infty)},$$

$$Sh_x = \frac{xJ_w}{D_B(C_w - C_\infty)} \qquad (13)$$

The set of ordinary differential equations (8) – (10) are highly non-linear, and therefore cannot be solved analytically. The finite-element method [23, 24] has been implemented to solve these non-linear equations.

3. Numerical method of solution

3.1. The finite-element method

The finite-element method (FEM) is such a powerful method for solving ordinary differential equations and partial differential equations. The steps involved in the finite-element are as follows.

(i) Finite-element discretization

(ii) Generation of the element equations

(iii) Assembly of element equations

(iv) Imposition of boundary conditions

(v) Solution of assembled equations

4. RESULTS AND DISCUSSION

Numerical investigation of the boundary value problem (8) – (10) together with boundary conditions (11) are conducted for different values of the key parameters that describe the flow characteristics and the results are illustrated graphically from Figs. 2 – 18. Comparison with previously published work is made and is shown in table 1. It is noticed from these figures 2 - 4 that the hydrodynamic boundary layer thickness decelerates whereas thermal boundary layer thickness and solutal boundary layer thickness heightens with enhance in the values of (*M*). It isnoticed from these figures 5 - 7that the thickness of all the hydrodynamic, thermal and solutal boundary layers depreciateswith increasing values of suction parameter (*V0 > 0*). However, the exact reverse trend is noticed in the velocity and temperature profiles and is depicted in Fig.8 and 9 with the values of injection parameter (*V0 < 0*).The velocity profiles rises with higher values of thermophoretic parameter (*Nt*) (Fig.10). Furthermore, both temperature and concentration profiles elevate in the boundary layer region for the higher values of thermophoretic parameter (*Nt*) (Figs 11 & 12). It is noticed that, with the increasing values of Brownian motion parameter (*Nb*), the temperature and concentration profiles are both decelerated in the fluid regime (Fig .13 & 14). Clearly, we noticed that Brownian motion parameter has significant influence on both temperature and concentration profiles.It can see from fig 15 that the thickness of hydrodynamic boundary layer is reduced with the enhancing values of (*Nr*). The temperature profiles of the fluid increases with increasing values of buoyancy ratio parameter (*Nr*). This is from the reality that higher the values of buoyancy ratio parameter enhance the fluids temperature, so that thermal boundary layer thickness is increased (Fig 16). It is observed that concentration distributions decelerate with the increasing values of the Lewis number in the entire boundary layer region (Fig. 17).

The values of skin-friction coefficient $\left(-f''(0)\right)$, Nusselt number $\left(-\theta'(0)\right)$ and Sherwood number $\left(-\phi'(0)\right)$ are calculated for diverse values of the parameters entered into the problem when the cone surface is hot and are shown in Table 2. It is evident from this table that the rate of velocityand the dimensionlessmass transfer rates are both enhances, whereas the rates of dimensionlessheat transfer decelerates with the increasing values of magnetic parameter (*M*). Therates of dimensionless rates of velocity, rates of dimensionlessheat and mass transfer are decelerates with an increment in the values of (*Nt*) in the entire boundary layer region. The rate of change of velocity, heat and mass transfer rates enhances with the higher values of Brownian motion parameter (*Nb*).

5. Conclusion

The impact of suction/injection and chemical reaction on natural convection boundary layer flow, heat and mass transfer along a vertical cone embedded in porous medium saturated by nanofluid with thermal radiation is numerically analyzed in this article. The slip of the flow in this problem is because of Brownian motion and thermophoresis. The powerful mathematical tool similarity variables approach is applied to convert the governing partial differential equations into the set of ordinary differential equations. The important results of the present study can be summarized as follows. The velocity profiles deteriorate, whereas, the temperature distributions are elevates with the higher values of magnetic parameter (*M*).With the higher values of values of thermophoretic parameter (*Nt*), the temperature distributions of the fluid rises.A rise in Brownian motion parameter (*Nb*) improves the heat transfer rate.

References

[1] S.U.S. Choi, and J.A. Eastman, Enhancing thermal conductivity of fluids with nanoparticles, *Proceedings of the ASME International Mechanical Engineering Congress and Exposition*, 66, 1995, pp. 99 – 105.

[2] Y. Li, J. Zhou, S. Tung, E. Schneider, and S. Xi, A review on development of nanofluid preparation and characterization, *Powder Technology*, 196(2), 2009, pp. 89 - 101.

[3] A. Ghadimi, R. Saidur, and H.S.C. Metselaar, A review of nanofluid stability properties and characterization in stationary conditions, *Int. J. Heat Mass Transfer*, 54, 2011, pp. 4051 – 4068.

[4] E. Abu-nada, Effects of variable viscosity and thermal conductivity of Al_2O_3–water nanofluid on heat transfer enhancement in natural convection, *International Journal of Heat and Fluid Flow*, 30, 2009, pp.679 – 690.

[5] S. Parvin, R. Nasrin, M.A..Alim, N.F. Hossain, and A.J. Chamkha, Thermal conductivity variation on natural convection flow of water–alumina nanofluid in an annulus, *Int. J. Heat Mass Transfer*, 55, 2012, pp. 5268 – 5274.

[6] J. Buongiorno, Convective transport in nanofluids, *J Heat Transfer*, 128, 2006, pp. 240 – 250.

[7] A.V. Kuznetsov, and D.A. Nield, Natural convective boundary-layer flow of a nanofluid past a vertical plate, *International Journal of Thermal Sciences*, 49, 2010, pp. 243 – 247.

[8] A.V. Kuznetsov, and D.A. Nield, Natural convective boundary-layer flow of a nanofluid past a vertical plate: A revised model, *International journal of thermal sciences*, 77, 2014, pp. 126 – 129.

[9] A. Aziz, and W.A. Khan, Natural convective boundary layer flow of a nanofluid past a convectively heated vertical plate, *Int. J. Therm. Sci.*, 52, 2012 pp. 83 – 90.

[10] A.J. Chamkha, A.M. Aly, and H. Al-Mudhaf, Laminar MHD mixed convection flow of a nanofluid along a stretching permeable surface in the presence of heat generation or absorption effects, *Int. J. MicroscaleNanoscale Thermal Fluid Transp.*, 2, 2011, pp. 51 – 70.

[11] M.M. Rashidi, N. Freidoonimehr, A. Hosseini, O. Anwar Bég, and T.K. Hung, Homotopy Simulation of Nanofluid Dynamics from a Non-Linearly Stretching Isothermal Permeable Sheet with Transpiration, *Meccanica*, 49 (2), 2014, pp. 469 – 482.

[12] A. Noghrehabadi, and A. Behseresht, Flow and heat transfer affected by variable properties of nanofluids in natural-convection over a vertical cone in porous media, *Comput. Fluids*, 88, 2013, pp. 313 – 325.

[13] A. Noghrehabadi, M.R. Saffarian, R. Pourrajab, and M. Ghalambaz, Entropy analysis for nanofluid flow over a stretching sheet in the presence of heat generation/absorption and partial slip, *Journal of Mechanical Science and Technology*, 27 (3), 2013, pp. 927 – 937.

[14] P. Sudarsana Reddy, and K.V. SuryanarayanaRao, MHD natural convection heat and mass transfer of Al_2O_3 - water and Ag - water nanofluids over a vertical cone with chemical reaction, *Procedia Engineering*, 127, 2015, pp. 476 – 484.

[15] A. Behseresht, A. Noghrehabadi, and M. Ghalambaz, Natural-convection heat and mass transfer from a vertical cone in porous media filled with nanofluids using the practical ranges of nanofluids thermo-physical properties, *Chemical Engineering Research and Design,* 92(3), 2013 pp. 447 – 452.

[16] R.S.R. Gorla, and A.J. Chamkha, Natural convective boundary layer flow over a horizontal

plate embedded in a porous medium saturated with a nanofluid, *J.Mod.Phys.*, 2, 2011 pp. 62 – 71.

[17] A.J. Chamkha, A.M.Rashad, and Ch. RamReddy, P.V. Murthy, Effect of Suction/Injection on Free Convection along a Vertical Plate in a Nanofluid Saturated Non- Darcy Porous Medium with Internal Heat Generation, *Indian Journal of Pure and Applied Mathematics*, 45, 2014 pp. 321 – 341.

[18] A.J. Chamkha, S. Abbasbandy, and A.M. Rashad, Non-Darcy Natural Convection Flow of Non-Newtonian Nanofluid Over a Cone Saturated in a Porous Medium with Uniform Heat and Volume Fraction Fluxes, *International Journal of Numerical Methods for Heat and Fluid Flow*, 25, 2015, pp.422 – 437.

[19] F. Garoosi, L. Jahanshaloo, M.M. Rashidi, A. Badakhsh, and M.A. Ali, Numerical Simulation of Natural Convection of the Nanofluid in Heat Exchangers using a Buongiorno Model, *Applied Mathematics and Computation,* 254, 2015, pp. 183 – 203.

[20] P. Sudarsana Reddy, and A.J. Chamkha, Influence of size, shape, type of nanoparticles, type and temperature of the base fluid on natural convection MHD of nanofluids, *Alexandria Eng. J.*, 55, 2016, pp. 331 – 341.

[21] D. Ruchika, PuneetRana, and Lokendra Kumar., MHD mixed convection nanofluidflowand heat transfer over an inclined cylinder due to velocity and thermal slip effects: Buongiorno's model, *Powder Technology*, 288, 2016, pp. 140 - 150.

[22]E. Haile, and B. Sankar, Effects of radiation, viscous dissipation, and magnetic field on nanofluid flow in a saturated porous media with convective boundary condition, *Computational Thermal Sciences:An International Journal*, 8, 2016, pp.177 – 191.

[23] PuneetRana, and R. Bhargava, "Flow and heat transfer of a nanofluid over a nonlinearly stretching sheet: a numerical study", Comm. Nonlinear Sci. Numer. Simulat.,**17**, pp. 212 – 226, 2012.

[24] P. Sudarsana Reddy, and A.J. Chamkha, Soret and Dufour effects on MHD convective flow of Al_2O_3–water and TiO_2–water nanofluids past a stretching sheet in porous media with heat generation/absorption, *Advanced Powder Technology,* 27, 2016, pp.1207 – 1218.

IJREAT International Journal of Research in Engineering & Advanced Technology, Volume 5, Issue 5, Oct - Nov, 2017
ISSN: 2320 – 8791 (Impact Factor: 2.317)
www.ijreat.org

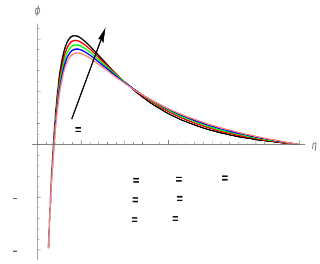

Fig.4. Effect of (M) on Concentration profiles.

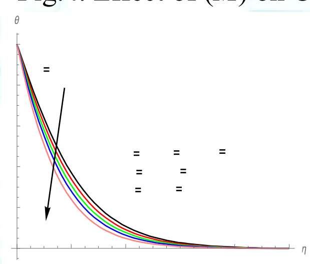

Fig.6. Effect of ($V0>0$) on Temperature profiles.

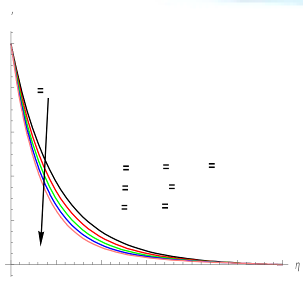

Fig.2. Effect of (M) on Velocity profiles.

ISSN: 2320 – 8791 (Impact Factor: 2.317)
www.ijreat.org

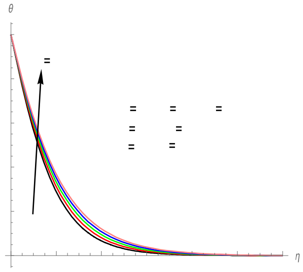

Fig.3. Effect of (*M*) on Temperature profiles.

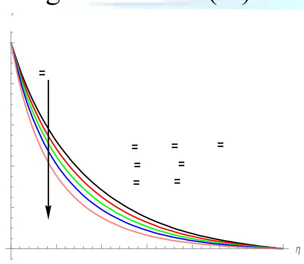

Fig.5. Effect of (*V0>0*) on Velocity profiles.

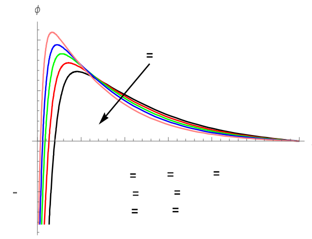

Fig.7. Effect of (*V0>0*) on Concentration profiles.

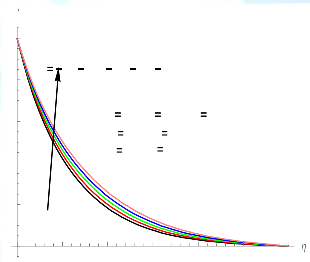

Fig.8. Effect of (*V0<0*) on Velocity profiles.

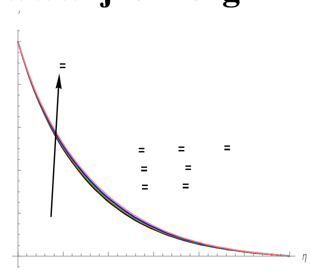

Fig.10. Effect of (*Nt*) on Velocity profiles.

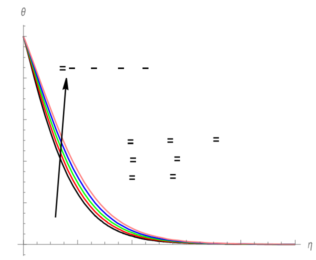

Fig.9. Effect of (*V0<0*) on Temperature profiles.

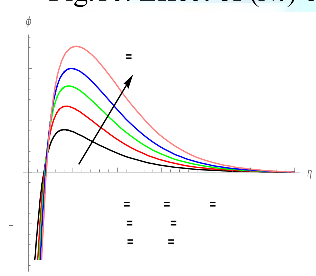

Fig.12. Effect of (*Nt*) on Concentration profiles.

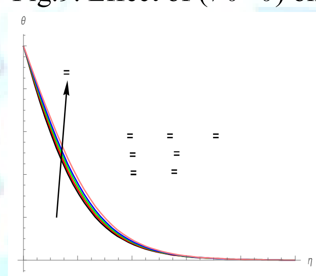

Fig.11. Effect of (*Nt*) on Temperature profiles.

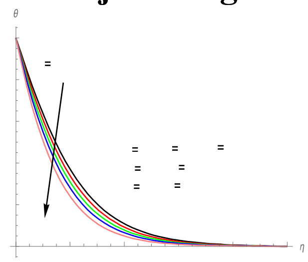

Fig.13. Effect of (*Nb*) on Temperature profiles.

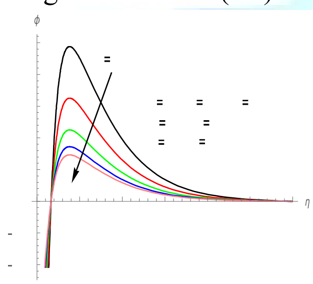

Fig.14. Effect of (*Nb*) on Concentration profiles.

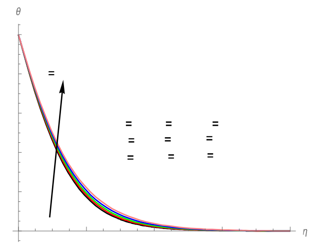

Fig.16. Effect of (*Nr*) on Temperature profiles.

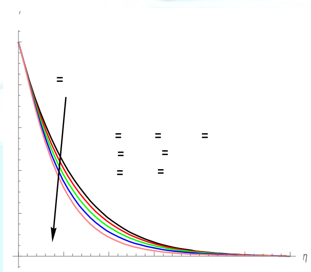

Fig.15. Effect of (*Nr*) on Velocity profiles.

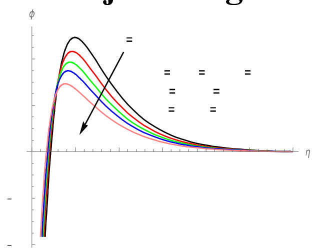

Fig.17. Effect of (Le) on Concentration profiles.

Table 1. Comparison of $\left(-\theta'(0)\right)$ and $\left(-\phi'(0)\right)$ for $\gamma = 0$(plate) and for different values of (Nr).

$-\theta'(0)$			$-\phi'(0)$	
Nr	Gorla*et al.* [16]	Present Study	Gorla*et al.* [16]	Present Study
0.0	0.32790	0.32784	1.49867	1.49781
0.1	0.32633	0.32598	1.48416	1.48394
0.2	0.32462	0.32405	1.46816	1.46789
0.3	0.32244	0.32229	1.45266	1.45214
0.4	0.32093	0.32125	1.43639	1.43598
0.5	0.31859	0.31868	1.41950	1.41938

Table 2. The values of skin-friction coefficient $\left(-f''(0)\right)$, Nusselt number $\left(-\theta'(0)\right)$ and Sherwood number $\left(-\phi'(0)\right)$ for different values of M, R, Nt, Nb, Cr.

M	Nt	Nb	$-f''(0)$	$-\theta'(0)$	$-\phi'(0)$

0.1	0.1	0.1	1.017437	0.480876	−0.48087
0.4	0.1	0.1	1.152343	0.460754	−0.46075
0.7	0.1	0.1	1.274794	0.443162	−0.44316
1.0	0.1	0.1	1.387420	0.427637	−0.42763
0.5	0.1	0.1	0.736263	0.441774	−0.44177
0.5	0.4	0.1	0.726170	0.418125	−1.67250
0.5	0.7	0.1	0.716200	0.396002	−2.77201
0.5	1.0	0.1	0.706376	0.375321	−3.75321
0.5	0.1	0.1	0.856428	0.648277	−0.10420
0.5	0.1	0.3	0.859613	0.662327	−0.06947
0.5	0.1	0.5	0.861573	0.670975	−0.04809
0.5	0.1	0.7	0.862611	0.675551	−0.03678